

# RSC Advances



This is an *Accepted Manuscript*, which has been through the Royal Society of Chemistry peer review process and has been accepted for publication.

*Accepted Manuscripts* are published online shortly after acceptance, before technical editing, formatting and proof reading. Using this free service, authors can make their results available to the community, in citable form, before we publish the edited article. This *Accepted Manuscript* will be replaced by the edited, formatted and paginated article as soon as this is available.

You can find more information about *Accepted Manuscripts* in the [Information for Authors](#).

Please note that technical editing may introduce minor changes to the text and/or graphics, which may alter content. The journal's standard [Terms & Conditions](#) and the [Ethical guidelines](#) still apply. In no event shall the Royal Society of Chemistry be held responsible for any errors or omissions in this *Accepted Manuscript* or any consequences arising from the use of any information it contains.

## ARTICLE

# Polytriazole Bridged with 2,5-Diphenyl-1,3,4-Oxadiazole Moieties: A Highly Sensitive and Selective Fluorescence Chemosensor for Ag<sup>+</sup>

FCite this:  
10.1039/x0xx00000x

DOI:

Shoupeng Cao, Zhichao Pei, Yongqian Xu, Ruina Zhang, Yuxin Pei\*

Received 00th January 2012,  
Accepted 00th January 2012

DOI: 10.1039/x0xx00000x

[www.rsc.org/](http://www.rsc.org/)

Fluorescent conjugated polytriazoles (FCP 1 - 4) containing both 2,5-diphenyl-1,3,5-oxadiazole (OXD) and 1,2,3-triazole moieties in the main chain were synthesized from aromatic diazide (**1**) and dialkynes (**2** - **5**) via click polymerization, respectively. In the polymers, OXDs (fluorophores) and triazole rings (generated via CuAAC acting as metal ion ligands) comprise a fluorescent system. The polytriazoles displayed relatively strong emission with quantum yield in a range of 0.20 – 0.28 at room temperature in DMF. The study on their ion-responsive properties showed that, although all four FCPs have good selectivity for Ag<sup>+</sup>, the intergration of bulky alkoxy side groups (methoxy for FCP 2, hexyloxy for FCP 3 and 2-ethylhexyloxy for FCP 4) to the main chain of the polytriazoles decreased their sensitivity for Ag<sup>+</sup> via alteration of polymer aggregation status and electron density of the main chain. Thus FCP 1 is highly sensitive for Ag<sup>+</sup>, where its  $K_{sv}$  is as high as  $1.44 \times 10^5 \text{ M}^{-1}$  and its lowest detection limit is in the ppb range ( $4.22 \times 10^{-7} \text{ M}$ ). This study provides an efficient click approach to the synthesis of a novel fluorescence sensor for Ag<sup>+</sup> detection, which could expand the application of click polymerization in designing fluorescence sensor based on triazole unit.

## Introduction

The widespread applications of silver and its compounds in electric, photographic, and pharmaceutical industries has led to a large amount of silver release into the environment from industrial wastes and emissions. As one of highly toxic heavy metal ions, the excess silver ions causes bioaccumulation and toxicity,<sup>1</sup> inactivation of sulfhydryl enzymes,<sup>2</sup> and irreversible darkening of the skin. In the past decades, the upsurge of silver nanoparticles (Ag-NPs), extensively applied in medicine, environmental remediation, and information technology, causes direct Ag-NPs release into environmental systems.<sup>3</sup> In the presence of moisture, oxidation of Ag-NPs results in the release of Ag<sup>+</sup> ions. The relative environmental concerns are therefore more pressing than ever, thus the development of selective and sensitive fluorescent chemosensors for Ag<sup>+</sup> is highly desirable. To date, the majority of fluorescence sensors for Ag<sup>+</sup> ions have been based on small or single molecule dyes.<sup>4-6</sup> Few literatures have reported fluorescent sensors based on conjugate polymers for silver-ion detection.<sup>7-9</sup>

Compared to small molecule sensors,<sup>10,11</sup> fluorescent conjugated polymer chemosensors for metal ions are increasingly attractive to researchers due to their advantages from enhancements associated with electronic communication between receptors along polymer backbones, processability,

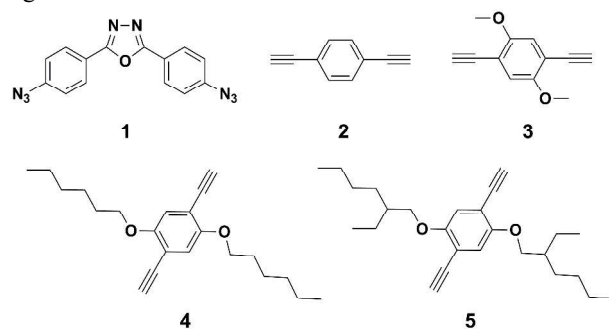
and feasibility to tune the electronic structure to change or enhance the selectivity of the system.<sup>12</sup>

Click polymerization, which originates from click reaction coined by Sharpless in 2001,<sup>13</sup> has become a powerful polymerization technique for new materials with tailored functionalities, where most often is carried out between di- or multiazides and di- or multialkynes with Cu(I) as catalyst (copper catalyzed alkyne-azide cycloaddition, CuAAC).<sup>14,15</sup> Thus, polytriazoles (PAs, named after the formation of the unique structural units of N-containing five-member 1,2,3-triazole ring from azide-alkyne cycloaddition) have been synthesized as highly efficient fluorescent polymer liquid crystal,<sup>15</sup> semiconductors,<sup>16</sup> hyper-cross-linked fluorescent polymer nanoparticles for cell imaging,<sup>17</sup> and highly sensitive fluorescent chemosensor for nitroaromatic explosives,<sup>18,19</sup> by incorporating chosen functional groups. Most attractively, numerous 1,2,3-triazole structural units along polymer backbones can act as potentially versatile ligands for metal coordination<sup>20</sup> and produce the “molecular wire effect”<sup>21</sup> for sensing signal amplification when used as optical sensors for metal ions. Moreover, by using a clickable monomer containing a fluorophore, a fluorescent PA with high sensitivity can be obtained. This extraordinary property, arising from the large numbers of both binding sites and fluorophores, allows efficient interaction with the target ions or molecules. Hence, a few PA-

based fluorescent sensors selective for  $\text{Hg}^{2+}$  were synthesized by Zhu and his coworkers.<sup>22-24</sup> Incorporating benzo[2,1,3]thiadiazole moieties to PA, the same researchers successfully synthesized a fluorescent polymer for  $\text{Ni}^{2+}$  with detection limit as low as  $1.1 \times 10^{-7} \text{ M}$ .<sup>25</sup> However, to the best of our knowledge, there is no polytriazole fluorescent chemosensor for  $\text{Ag}^+$  reported.

On the other hand, 1,3,4-oxadiazole unit with electron-deficient nature is well known for their high electron affinity values and excellent electron-transporting properties, and is a very popular chromophore in polymers for photonic devices, such as OLEDs,<sup>26</sup> polymer light-emitting diodes,<sup>27</sup> and photovoltaic cells.<sup>28</sup> Polymers containing 1,3,4-oxadiazole units endow the final polymer not only high thermo-stability and chemical stability, but also high photoluminescence efficiency.<sup>29</sup> For instance, Cheng and his coworkers synthesized linear chiral polymers based on optically active polybinaphthyls and 1,3,4-oxadiazole, which showed strong green-blue fluorescence.<sup>30</sup> Although the polymers showed excellent sensitivities when used as fluorescent chemosensor for metal ions, no selectivity was observed: the polymers showed similar quenching efficiencies for  $\text{Ni}^{2+}$ ,  $\text{Cu}^{2+}$ ,  $\text{Pb}^{2+}$ ,  $\text{Zn}^{2+}$ ,  $\text{Hg}^{2+}$ , and  $\text{Ag}^+$ . Moderate coordination ability of  $\text{Ag}^+$  and the strong interferes of  $\text{Hg}^{2+}$  and other heavy metal ions make  $\text{Ag}^+$  difficult to be discriminated from other chemically similar heavy metal ions.<sup>6,7</sup> The design and synthesis of highly sensitive and selective system for the determination of trace amount of silver ions remains a challenge.

In this work, by using 2,5-bis(4-azidophenyl)-1,3,4-oxadiazole (**1**) as diazide monomer, and 1,4-diethynylbenzene (**2**), 1,4-diethynyl-2,5-bis(methoxyl)benzene (**3**), 1,4-diethynyl-2,5-bis(hexyloxy)benzene (**4**), and 1,4-diethynyl-2,5-bis(2-ethylhexyloxy)benzene (**5**) as dialkynyl monomers (Scheme 1), novel fluorescent polytriazoles containing both units of 1,2,3-triazole and 1,3,4-oxadiazole were first synthesized via click polymerization (CuAAC). Thereafter, the polytriazoles were characterized by FTIR, GPC, TGA, and DSC, respectively. Their fluorescence property, selectivity, and sensitivity for heavy metal ions were investigated. To our delight, we found that FCP 1 (fluorescent conjugated polytriazole formed with monomer **1** and **2**) showed excellent selectivity and sensitivity for  $\text{Ag}^+$ .



**Scheme 1** The structures of monomers used for click polymerization.

## Results and Discussion

To synthesize polytriazoles bridged with 2,5-diphenyl-1,3,4-oxadiazole (OXD) moieties via click polymerization, diazide monomer 2,5-bis(4-azidophenyl)-1,3,4-oxadiazole (**1**) and dialkyne monomers 1,4-diethynylbenzene (**2**), 1,4-diethynyl-2,5-bis(methoxyl)benzene (**3**), 1,4-diethynyl-2,5-bis(hexyloxy)benzene (**4**), and 1,4-diethynyl-2,5-bis(2-ethylhexyloxy)benzene (**5**) were obtained first according to the published procedures (Scheme 2a - c).<sup>31-37,55</sup> Monomer **1** was designed to contain a 1,3,4-oxadiazole unit for incorporating it to the polymer backbone later via click polymerization. Clickable functional groups of azide and alkyne were chosen specifically for performing CuAAC reaction to generate 1,2,3-triazole unit. Methoxyl, *n*-hexyloxy and 2-ethylhexyloxy groups were introduced to monomer **3**, **4** and **5**, respectively, to obtain polytriazoles with side chains in order to study their influence on solubility, aggregation, and fluorescent properties. Thus, via click reaction between azide and alkyne groups, four FCPs were synthesized: FCP 1 was from **1** and **2**, FCP 2 from **1** and **3**, FCP 3 from **1** and **4**, FCP 4 was from **1** and **5**, respectively, in DMF in the presence of  $\text{Cu}(\text{PPh}_3)_3\text{Br}$ .<sup>15</sup> Both units of oxadiazole and triazole were incorporated into the polymer backbones. After precipitation, washing, and drying steps, FCP 1, FCP 2, FCP 3, and FCP 4 were obtained with a yield of 37 %, 49 %, 61 %, and 67 %, respectively, as yellowish solids.

It's worthy to mention that the residual copper in the final polymers from the catalyst  $\text{Cu}(\text{PPh}_3)_3\text{Br}$  used in the polymerization is rather low (roughly equal to 0.1equiv.),<sup>38</sup> the quenching caused by it is little and can be ignored (see Fig. S14).

The polymers were characterized by GPC, FTIR, TGA, and DSC, respectively.

FCPs	$M_n (\times 10^3)$	$M_w (\times 10^3)$	PDI	$T_d (^\circ\text{C})$
FCP 1	3.78	5.7	1.51	289
FCP 2	5.24	6.9	1.32	204
FCP 3	11.6	14.5	1.24	273
FCP 4	12.0	18.0	1.50	239

**Table 1** The characteristic data of FCP 1 – 4 from GPC and TGA.

The number-average molecular weights ( $M_n$ ), the weight-average molecular weights ( $M_w$ ), and polydispersity indexes (PDI) of FCPs were determined by GPC using polystyrene standards in DMF (Table 1). It can be seen that the polymers synthesized in this work have moderate molecular weights and acceptable PDIs: 3780 and 1.51 for FCP 1, 5240 and 1.32 for FCP 2, 11600 and 1.24 for FCP 3, and 12000 and 1.50 for FCP 4. A noteworthy observation is the molecular weights of FCP 3 and 4, which are much higher than FCP 1 under the same polymerization conditions, potentially as a result of the synergetic effect of higher monomer reactivity of **4** and **5** due to the electron-donating bulky alkoxy groups at ortho-position of benzene ring and better solubility of comb oligomers formed during the polymerization processes.

The click polymerization between azide and alkynyl groups (monomer **1** and **2**) was followed by NMR for 2 h. The  $^1\text{H}$  NMR spectra of the starting materials and the reaction mixture after 2 h was recorded and shown in Fig. S1. It can be seen that a new peak appeared at 9.56 ppm, attributed to the proton in the new-generated triazole ring. In the meantime, the integration of the peak at 4.38 ppm ( $\text{HC}\equiv\text{C}$ -) decreased with time, indicating a consumption of alkynyl groups with reaction and a successful click reaction between monomer **1** and **2**.

The FTIR spectrum of FCP **1** is shown in Fig. 1. Compared to the IR spectra of monomer **1** and **2**, a new absorption peak at  $3106\text{ cm}^{-1}$  was observed, which is assigned to the stretching vibration of C-H on triazole ring formed in click polymerization.<sup>39</sup> The sharp absorption band of  $\text{C}=\text{N}-\text{N}=\text{C}$  in monomer **1**<sup>40</sup> at  $1490\text{ cm}^{-1}$  deformed slightly due to the stretching vibrations of  $\text{C}=\text{C}$ ,  $\text{N}=\text{N}$ , and triazole ring at  $1508\text{ cm}^{-1}$ .<sup>40-43</sup> Although the stretching vibrations of C-H ( $3296\text{ cm}^{-1}$ ) in alkyne and azide ( $2092\text{ cm}^{-1}$ ) in the polymer were still observed, the relative intensities of azide to  $\text{C}=\text{N}$  in OXD unit ( $1610\text{ cm}^{-1}$ )<sup>40, 41</sup> and  $\text{C}\equiv\text{CH}$  decreased significantly. A similar phenomenon was also observed in the IR spectra of FCP **2**, **3**, and **4**, though the intensity decrease was even more significant (Fig. S2, S3, and S4) due to the lower percentages of the residual end groups of azide and alkyne and higher DPs (degrees of polymerization) in FCP **2**, **3**, and **4** compared to FCP **1** (see Table 1). All these results indicated a successful click reaction had taken place between monomer **1** and **2** - **5**, respectively.

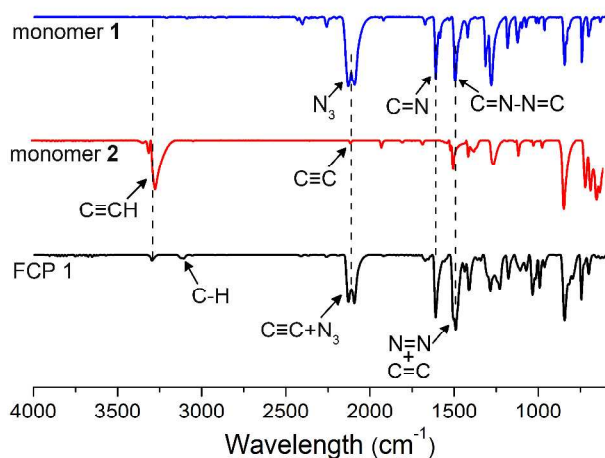


Fig. 1 FTIR spectra of monomer **1**, **2**, and FCP **1**.

Thermal properties of FCPs were evaluated by TGA and DSC under  $\text{N}_2$  atmosphere at a heating rate of  $10\text{ }^\circ\text{C min}^{-1}$ . According to the thermograms from TGA (Fig. 2), the four polymers had similar thermal stabilities: 5 % weight loss was observed at higher than  $200\text{ }^\circ\text{C}$ , and an apparently degradation was observed at temperature ranging from  $240\text{ }^\circ\text{C}$  to  $650\text{ }^\circ\text{C}$ . The temperatures for 5 % weight loss ( $T_d$ ) of FCP **1** - **4** is 289, 204, 273 and  $239\text{ }^\circ\text{C}$ , respectively (Table 1). While two endothermic peaks centered at  $\sim 180$  and  $\sim 320\text{ }^\circ\text{C}$  were recorded on the DSC thermograms of the FCPs (Fig. S5). We speculated that the peak at  $180\text{ }^\circ\text{C}$  could be attributed to the deterioration of small segments or terminal groups, corresponding to the temperature for less than 5 % weight loss on TGA thermograms. Since the obvious weight loss of the FCPs occurred after  $300\text{ }^\circ\text{C}$

(see Fig. 2), it is thus reasonable to assign the second peak at  $\sim 320\text{ }^\circ\text{C}$  to the thermal decomposition of the polymer skeletons. The results showed that the polymers possess desirable thermal properties, which most likely can be attributed to the multi-ring structure on the main chains of the polymers, although the side groups (methoxyl for FCP **2**, hexyloxy for FCP **3**, and 2-ethylhexyloxy for FCP **4**) impaired the thermostability of the polymers to some extent, as shown in Fig. 2 and Fig. S5.

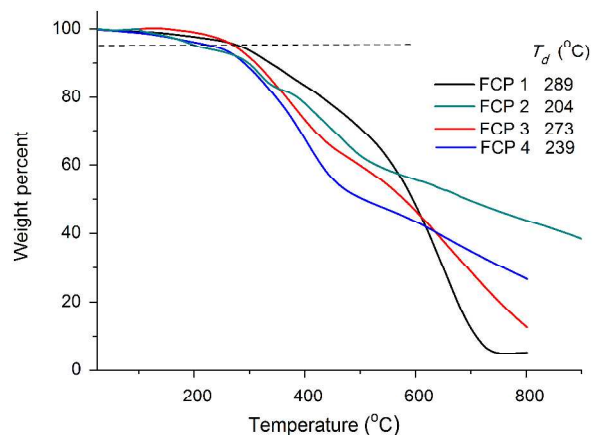
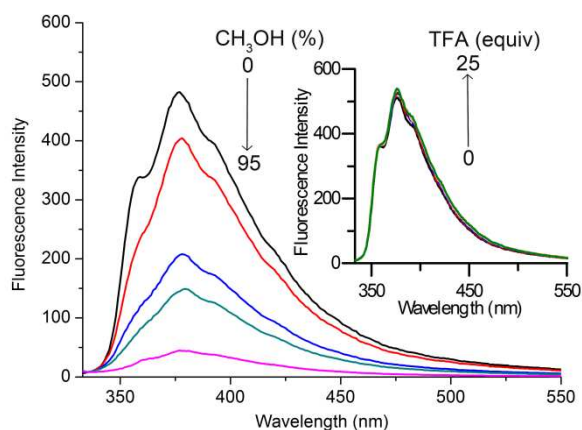


Fig. 2 TGA curves of FCP **1** - **4**.

FCPs are nonfluorescent in solid state. However, under UV light ( $\lambda_{\text{ex}} = 365\text{ nm}$ ), FCPs showed blue-green fluorescence in common aprotic organic solvents such as dichloromethane, THF, chloroform, acetonitrile, DMF, and DMSO. While in protic solvent methanol, no fluorescence was observed. It is well-known that alcohols can form intermolecular hydrogen-bonded complex with small fluorescent molecules to produce profound effect on their fluorescent behavior.<sup>44</sup> However, few reports were found to discuss the effect of methanol on emission of conjugated fluorescent polytriazoles (CPAs): Buzn and his co-workers reported that methanol had no alteration of the emission of poly(arylenetriazolyene)s, while addition of acid to the polymers caused a red shift, which was attributed by the authors to conformation changes by protonation of triazole rings.<sup>16</sup> In the other study, a mixture of methanol/water (1:1, v/v) was used as solvent to dissolve CPA to investigate the quenching efficiency of  $\text{Hg}^{2+}$ .<sup>24</sup> Based on these reports, it is interesting to further investigate the fluorescent behaviour of FCPs upon the addition of methanol and acid. The results are displayed in Fig. 3. It can be seen that the fluorescence intensity of FCP **1** in DMF decreased gradually with increasing percentage of methanol. On the other hand, a slight increase of fluorescence intensity (4 % upon 25 equiv.) was observed when FCP **1** in DMF was titrated with trifluoroacetic acid (TFA). This suggested that the increase of methanol in the solution caused stronger aggregation of the macromolecules and  $\pi$ -stacking interaction between neighbouring polymer chains, which in the end led to the fluorescence quenching of FCPs. On the other hand, protonation of triazole rings by TFA afforded the polymer chains to be positively charged, which kept them from aggregation and the homogeneity of the solution was enhanced. This is why a slight increase in emission intensity was observed.



**Fig. 3** Fluorescence intensity of FCP 1 (46  $\mu\text{M}$ , corresponding to the triazole unit) in DMF upon the addition of  $\text{CH}_3\text{OH}$  and TFA (inset),  $\lambda_{\text{ex}} = 323 \text{ nm}$ .

The quantum yield of emission ( $\Phi_f$ ) of FCPs in DMF was 0.20, 0.24, 0.22, and 0.28 for FCP 1, 2, 3, and 4, respectively, with reference to quinine sulfate in 0.5 mol/L  $\text{H}_2\text{SO}_4$  solution, which was calculated according to the literature method, as shown in Eqn. S1.<sup>45</sup> The UV-Vis absorption and fluorescent properties of FCPs in DMF were studied by UV-Vis and fluorescence spectroscopies, respectively. The results are shown in Fig. 4. UV-Vis spectra of FCPs in DMF disclosed the absorption maximum was 323 nm for FCP 1, 347 nm for FCP 2, 365 nm for FCP 3, and 340 nm for FCP 4, respectively. The analysis by fluorescence spectroscopy showed that the emission maximum of FCP 1 in DMF appeared at 373 nm with a shoulder at 359 nm under an excitation of 323 nm, while for FCP 2, 3, and 4, the emission maxima appeared at 498 nm, 489 nm, and 493 nm, respectively. Compared to the Stoke shift of FCP 1 (50 nm), FCP 2, 3 and 4 gave a much larger Stoke shift, 151 nm, 124 nm, and 153 nm, respectively. Besides, the vibrational structure observed in the emission spectrum of FCP 1 disappeared in the emission spectra of FCP 2 – 4.

Considering the shoulder in the emission spectrum of FCP 1 disappeared with the addition of methanol (Fig 3), we surmise that the shoulder corresponds to the isomers resulted from proton transfer due to the intramolecular hydrogen bonds in FCP 1, which were broken by the intermolecular hydrogen bonds formed between FCP 1 and methanol. The lack of the intramolecular hydrogen bonds in FCP 2 – 4, therefore no isomers formed in the solutions, could be the reason why the vibrational structure observed in the emission spectrum of FCP 1 disappeared in the emission spectra of FCP 2 – 4.<sup>46</sup>

The absorption maxima, emission maxima, Stoke shifts, and quantum yields of FCP 1, FCP 2, FCP 3, and FCP 4 are summarized in Table 2.

Polymer	$\lambda_{\text{abs-max}}$	$\lambda_{\text{em-max}}$	Stoke shift (nm)	$\Phi_f$
FCP 1	323	373	50	0.20
FCP 2	347	498	151	0.24
FCP 3	365	489	124	0.22
FCP 4	340	493	153	0.28

**Table 2** The absorption maxima, emission maxima, Stoke shifts, and quantum yields of FCP 1 - 4.

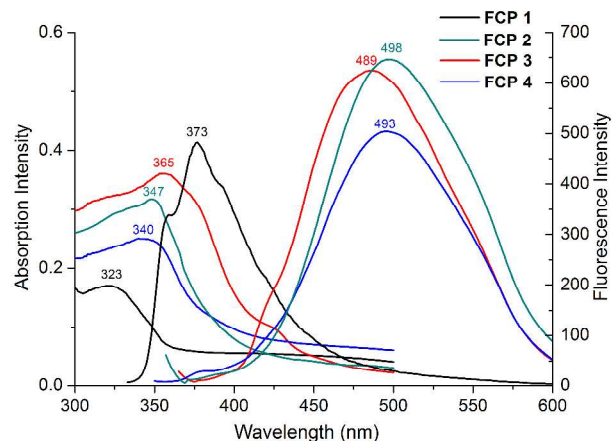


**Fig. 4** Absorption and fluorescence emission spectra of FCPs in DMF (con. of FCP 1, 2, 3, and 4 were 46, 41, 32, and 29  $\mu\text{M}$  corresponding to the triazole unit, respectively).

Bearing several donor sites, 1,2,3-triazoles, known since the end of the 19<sup>th</sup> century, are now versatile ligands for metal coordination.<sup>20</sup> FCPs synthesized via CuAAC in the present work, containing multi oxadiazole and triazole moieties, are expected to have distinctive metal ion responsive behaviors. The selectivity of FCPs for metal ions was examined by monitoring the change of fluorescence intensity upon the addition of various metal ions, including  $\text{Hg}^{2+}$ ,  $\text{Cu}^{2+}$ ,  $\text{Cr}^{3+}$ ,  $\text{Cd}^{2+}$ ,  $\text{Co}^{2+}$ ,  $\text{Mn}^{2+}$ ,  $\text{Ni}^{2+}$ ,  $\text{Pb}^{2+}$ ,  $\text{Zn}^{2+}$ ,  $\text{Ba}^{2+}$ ,  $\text{Mn}^{2+}$ ,  $\text{Ca}^{2+}$ ,  $\text{K}^+$ ,  $\text{Na}^+$ , and  $\text{Ag}^+$ . The results shown in Fig. 5 were obtained by using the solution of FCP 1 in DMF (46  $\mu\text{M}$ , corresponding to the triazole unit). It was found that the fluorescence intensity of the PA changed little in the presence of most metal ions examined (10 equiv., quantity related to corresponding triazole unit). Under the same conditions, the addition of  $\text{Cu}^{2+}$  resulted in a moderate decrease in fluorescence intensity. In contrast, FCP 1 responded to  $\text{Ag}^+$  significantly: its fluorescence intensity decreased by 95 % upon the addition of 1.0 equiv.  $\text{Ag}^+$ , and the quantum yield decreased to 0.03. We also studied the kinetics of the fluorescence behaviour by adding 1.0 equiv.  $\text{Ag}^+$  into FCP 1 solution. As shown in Fig. S6, the quenching of 90 % fluorescence intensity took about 200 seconds, indicating a fast response process.

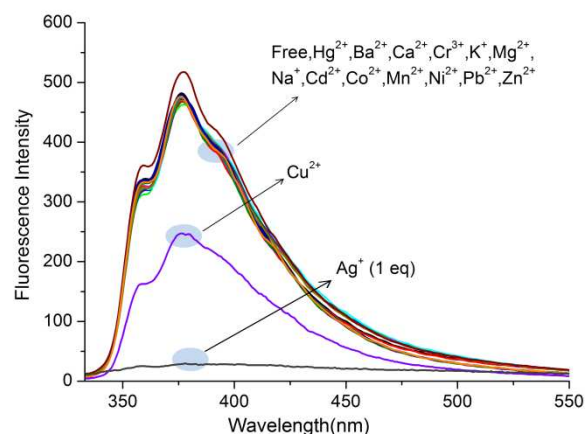


**Fig. 5** The selectivity of FCP 1 (46  $\mu\text{M}$ , corresponding to the triazole unit) towards  $\text{Ag}^+$  and other metal ions. The fluorescence measurement was taken

at  $\lambda_{\text{ex}} = 323$  nm in DMF at room temperature in the presence of metal ions (10 equiv. each, except  $\text{Ag}^+$ , which was 1.0 equiv.).

The high selectivity of FCP 1 towards  $\text{Ag}^+$  was based on the following features of  $\text{Ag}^+$  and the polytriazole: 1) The weak Lewis acidity of  $\text{Ag}^+$  endows a better affinity to the Lewis basic triazole rings;<sup>47</sup> 2) Silver ions has a strong coordination ability to electron-rich triazole moieties in the polymer backbone,<sup>20,48</sup> and the complexation induced the aggregation of the polymer which resulted in the fluorescence quenching.<sup>7</sup> Thus, combination of OXDs as fluorophores and triazole rings as metal ligands made FCP 1 an excellent fluorescent conjugate polymer sensor selectively for  $\text{Ag}^+$ . The quenching mechanism (Fig. 6) is believed to relate to the quenching behavior of energy transfer along the polymer backbones<sup>12</sup> and  $\text{Ag}^+$  induced aggregation effect.<sup>7</sup>

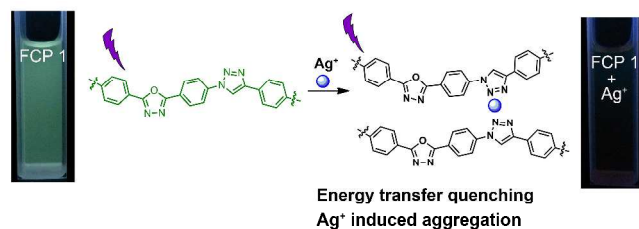


**Fig. 6** The illustration of the quenching mechanism exemplified with FCP 1 in the presence of  $\text{Ag}^+$  in DMF.

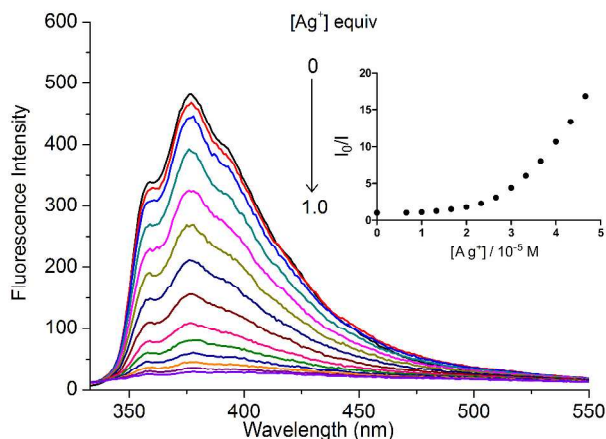


**Fig. 7** Fluorescence quenching of FCP 1 (46  $\mu\text{M}$ , corresponding to triazole unit) in DMF upon the addition of  $\text{Ag}^+$  with increasing concentrations (0 - 1 equiv.),  $\lambda_{\text{ex}} = 323$  nm.

As is evident from Fig. 7, obvious fluorescence quenching was observed upon the increasing addition of  $\text{Ag}^+$ . Coincidentally, green light from FCP 1 in DMF gradually disappeared, which was easily visible by the naked eye under UV light ( $\lambda_{\text{ex}} = 365$  nm).

The quenching process was analyzed by Stern-Volmer analysis according to the Stern-Volmer equation shown below:<sup>49,50</sup>

$$I_0/I = 1 + K_{\text{sv}}[Q]$$

Where  $I_0$  and  $I$  are the fluorescence intensities observed in the absence and presence of metal ions, respectively.  $Q$  is the quencher concentration.  $K_{\text{sv}}$  is the Stern-Volmer quenching constant and related to quenching efficiency. For a purely static quenching

process, plotting relative fluorescence intensity ( $I_0/I$ ) against the concentration of  $[Q]$  should produce a linear line, and the slope of the line equals to  $K_{\text{sv}}$  constant.<sup>51</sup> However, static and dynamic quenching very often occur simultaneously in the quenching processes of fluorescent conjugated polymer-metal ion system, resulting in a deviation of the quenching plot from Stern-Volmer linearity.<sup>12,24,52</sup> Thus, the steady-state emission Stern-Volmer analysis for FCP 1- $\text{Ag}^+$  interaction in DMF solution led to a positive deviation from the linear Stern-Volmer line (inset in Fig. 7). The averaged  $K_{\text{sv}}$  value of FCP 1 was  $1.44 \times 10^5 \text{ M}^{-1}$ , which is equally high as previous reported data for other excellent fluorescence conjugated polymer sensors,<sup>7,15,24,30,53</sup> and indicated that the polymer is highly sensitive to  $\text{Ag}^+$ . Calibration curve of FCP 1 was obtained from the plot of fluorescence intensity in the presence of  $\text{Ag}^+$  from 1 : 0 - 1 : 1.0 molar ratios (Fig. S7). Based on the curve, the lowest detection limit of the polymer FCP 1 to  $\text{Ag}^+$  was decided to be  $4.22 \times 10^{-7} \text{ M}$ , which is low enough for sensing sub-millimole concentration of  $\text{Ag}^+$  encountered practically.

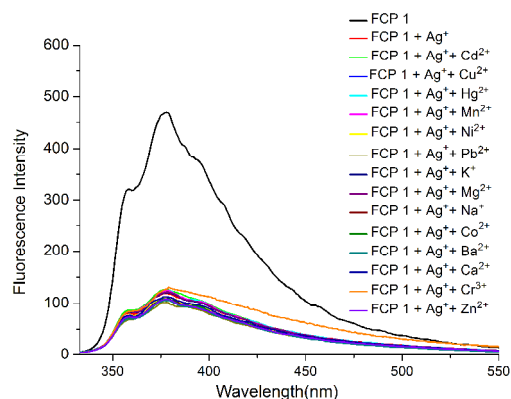


**Fig. 8** Metal specificity of FCP 1 (46  $\mu\text{M}$ , corresponding to the triazole) in DMF with a mixture of  $\text{Ag}^+$  and other metal ions ( $\text{Ag}^+$ : other metals = 1 : 5 in equiv.). The equivalent of  $\text{Ag}^+$  was kept for 0.6 equiv.,  $\lambda_{\text{ex}} = 323$  nm.

In addition to the prerequisites of high selectivity and sensitivity for an excellent fluorescence sensor, one more crucial requirement is minor or no disturbance from other metal ions. Thus, competition experiments were conducted by subjecting FCP 1 to appropriate mixtures of  $\text{Ag}^+$  and five folds of other various metal ions. Competition events were monitored by fluorescence spectroscopy. As shown in Fig. 8, less than 5 % deviations were observed from other metals interference, which proved that the polymer could show remarkable fluorescence quenching response to  $\text{Ag}^+$  without much interference from other metal ions. On the whole, the polytriazole bridged with 2,5-diphenyl-1,3,4-oxadiazole moieties in the main chain displayed fantastic response to  $\text{Ag}^+$  with high selectivity, and sensitivity, therefore can be used as a fluorescent chemosensor for detection of  $\text{Ag}^+$ .

To illustrate the potential application of FCPs, real water samples, such as tap water and water from Wutai reservoir, were used. Three concentrations of  $\text{Ag}^+$  were prepared and analysed using a DMF solution of FCP 1 (46  $\mu\text{M}$ , corresponding to the triazole unit). The data were shown in Table 3 and Fig. S8. Both water samples exhibited nice fluorescence response, the recovery yield is higher

than 91% and the deviation is in the acceptable range (1.1 % to 8.7 %).

Sample	T1	T2	T3	R1	R2	R3
$C_0$ ( $10^{-5}$ M)	1.166	2.000	2.833	1.166	2.000	2.833
$C_1$ ( $10^{-5}$ M)	1.179	2.086	2.873	1.065	1.893	2.672
Recovery (%)	101.1	104.3	101.4	91.3	94.7	94.3
SD ( $10^{-7}$ M)	2.666	2.913	5.666	1.041	2.585	5.229

**Table 3** The application of FCP 1 used to detect the concentration of  $Ag^+$  in real water samples. **T**: tap water; **R**: water from Wutai reservoir;  $C_0$ : Real concentrations of  $Ag^+$  added to the water samples;  $C_1$ : Detected concentrations of  $Ag^+$  by a DMF solution of FCP 1; SD: standard error.

Optoelectronic properties of fluorescent polymers would be influenced and governed bulky side groups tailed to the polymer backbone.<sup>7</sup> In addition, the electronic nature of side group changes the energy transfer of the polymer backbones, which is more relevant to the optoelectronic properties of the resultant polymers. To gain insight into the effects of side groups on the fluorescence behaviour of the polytriazoles synthesized in this work, methoxyl, n-hexyloxy, and 2-ethylhexyloxy groups tailed polymers FCP 2, FCP 3, and FCP 4 were investigated for comparison with FCP 1. The methoxyl, n-hexyloxy, and 2-ethylhexyloxy groups as not formally part of the conjugated network were expected to alter the energy transfer of the polymer backbone and minimize the aggregation of the macromolecules by interrupting the stacking of the polymer in solution, which affects the fluorescent properties of the polymers.

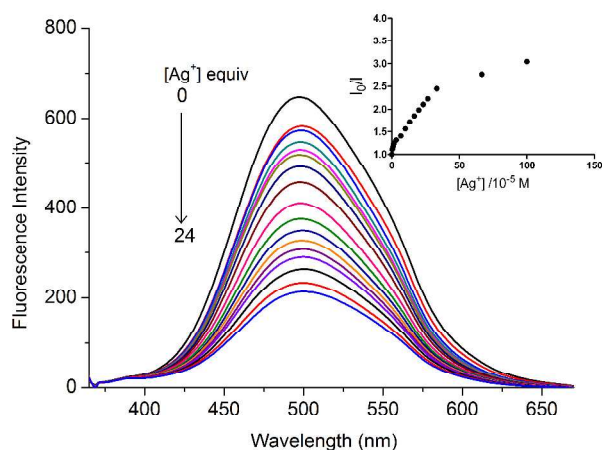


**Fig. 9** Fluorescence quenching of FCP 2 (41  $\mu$ M, corresponding to triazole unit) in DMF upon the addition of  $Ag^+$  with increasing concentrations (0 -24 equiv.),  $\lambda_{ex}$  = 347 nm.

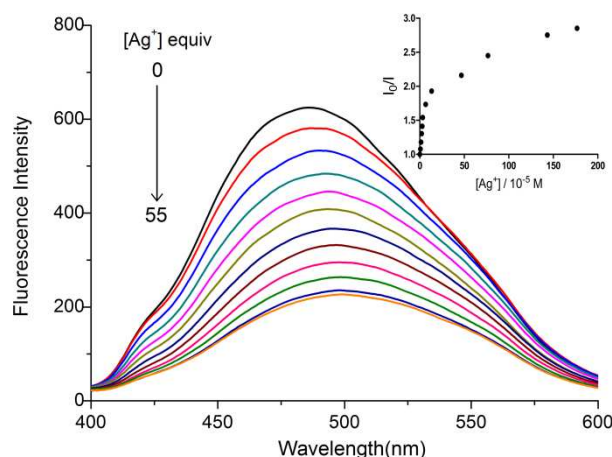


**Fig. 10** Fluorescence quenching of FCP 3 (32  $\mu$ M, corresponding to triazole unit) in DMF upon the addition of  $Ag^+$  with increasing concentrations (0 - 55 equiv.),  $\lambda_{ex}$  = 365 nm.

The selectivity and sensitivity of FCP 2, 3, and 4 were studied with similar conditions as used for FCP 1. Surprisingly, although FCP 2, 3, and 4 showed similar selectivity (Fig. S9, S10, and S11) as FCP 1, their sensitivity for  $Ag^+$  and  $Cu^{2+}$  decreased considerably: the addition of 10 equiv. of  $Ag^+$  could only quench 59 % fluorescence of FCP 2 (Fig. 9), 52 % fluorescence of FCP 3 (Fig. 10), and 43 % fluorescence of FCP 4 (Fig. 11), respectively; the addition of 10 equiv. of  $Cu^{2+}$  could only quench 5 % fluorescence of FCP 2 (Fig. S9), 15 % fluorescence of FCP 3 (Fig. S10), and 17 % fluorescence of FCP 4 (Fig. S11), respectively. In addition, the quenching plots of the three polymers are downward curvatures (insets in Fig. 9, 10, and 11), indicating that the quenching processes involved heterogeneous population, *i.e.* only a fraction of triazole moieties was accessible to the quencher.<sup>54</sup>

It has been proved that interchain interactions, which are less hindered by the less bulky alkoxyl side groups, promote energy transfer to lower energy chromophores,<sup>33</sup> and the ability of metal ions to completely quench the fluorescence polymer resulted from the electron-transfer interactions between the conjugated polymer backbone and metal ion.<sup>52</sup> Therefore, it is logical to speculate that the decreased sensitivity of FCP 2, 3, and 4 to the analytes and the difference of their quenching processes from that of FCP 1 are due to the side groups in the main chains of FCP 2 (methoxyl), FCP 3 (n-hexyloxy), and 4 (2-ethylhexyloxy), which altered the polymer aggregation status<sup>7</sup> and energy transfer in the backbone, and further influenced the fluorescence behavior of the resultant polymers.<sup>33</sup>

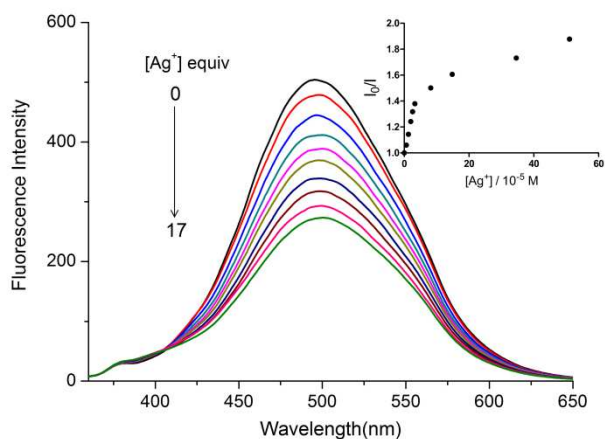


**Fig. 11** Fluorescence quenching of FCP 4 (29  $\mu\text{M}$ , corresponding to triazole unit) in DMF upon the addition of  $\text{Ag}^+$  with increasing concentrations (0 - 17 equiv.),  $\lambda_{\text{exc}} = 340 \text{ nm}$ .

## Conclusions

In summary, fluorescent conjugated polytriazoles (FCP 1 - 4) containing both 2,5-diphenyl-1,3,5-oxadiazole and 1,2,3-triazole moieties in the main chain were synthesized from aromatic diazide (**1**) and dialkynes (**2** - **5**) via click polymerization, respectively. In the particularly designed polymers, OXD moieties (acting as fluorophores<sup>31</sup>) and triazole rings generated via CuAAC (acting as metal ion receptors) comprise a fluorescent system. The study on their ion-responsive properties shows that, although all four FCPs have good selectivity on  $\text{Ag}^+$ , the integration of alkoxy side groups as not formally part of the conjugated network to the main chain of the polytriazoles can have significant effect on the optical properties of conjugated systems, which decreased their sensitivity for  $\text{Ag}^+$  via alteration of polymer aggregation status and energy transfer of the main chain. Moreover, FCP 1 as a highly sensitive and selective fluorescent chemosensor for  $\text{Ag}^+$  was obtained via rational design, where its  $K_{\text{sv}}$  is as high as  $1.44 \times 10^5 \text{ M}^{-1}$  and the lowest detection limit is in ppb range ( $4.22 \times 10^{-7} \text{ M}$ ). This study provides an efficient click approach to the synthesis of a novel fluorescence sensor for  $\text{Ag}^+$  detection, which could expand the application of the click polymerization in designing fluorescent sensor based on triazole unit.

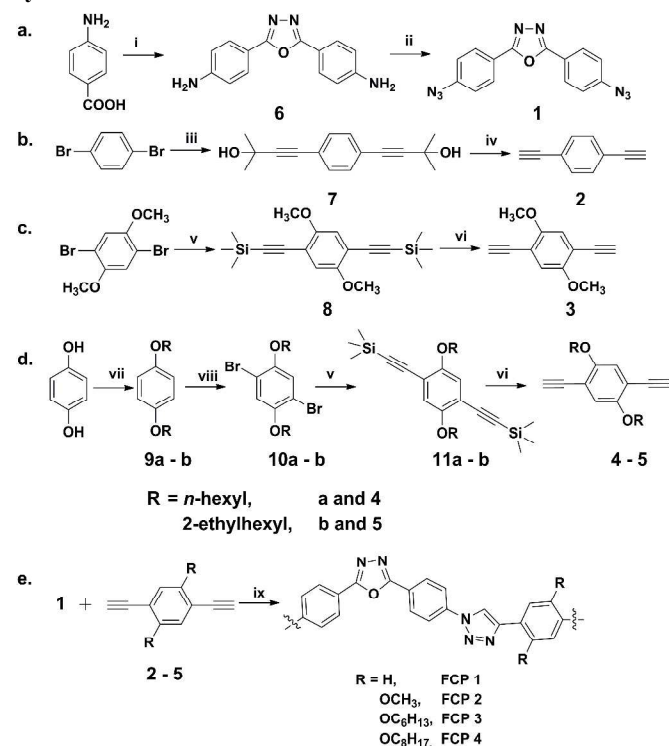
## Experimental Section

### Instruments and Materials

All the reagents were purchased from commercial suppliers and used without further purification. THF and  $\text{Et}_3\text{N}$  were purified by distillation in the presence of  $\text{CaH}_2$  before use. Other reagents and solvents were analytical grade and used as received. Flash chromatography was performed using silica gel with a grain size of 40-63  $\mu\text{m}$  (Qingdao Haiyang Co., Ltd) and hexane as eluent.  $^1\text{H}$  and  $^{13}\text{C}$  NMR spectra were recorded on a Bruker Advance 500 instrument in  $\text{CDCl}_3$ , using the residual signals from  $\text{CHCl}_3$  ( $^1\text{H}$ :  $\delta$  7.26 ppm;  $^{13}\text{C}$ :  $\delta$  77.0 ppm) as internal standard. UV-Vis spectra were obtained from Shimadzu UV-1750 and fluorescence spectra were obtained from Shimadzu RF-5301. Infrared spectra were recorded on an FTIR-instrument (BRUKER TENSOR 27) with KBr

pellets. Thermogravimetric analysis (TGA) thermograms were recorded on an auto-simultaneous measurement of thermogravimetry and differential thermal analysis (Shimadzu DTG-60A). Differential Scanning Calorimetry analysis (DSC) thermograms were recorded on TA DSC Q2000 instrument. Molecular weight was determined by gel permeation chromatography (GPC) with Waters-515 HPLC pump using DMF as solvent and compared to polystyrene standards. Metal ions such as nitrate salts or perchlorate salts were used to prepare metal ion stock solutions. 2,5-bis(*p*-aminophenyl)-1,3,4-oxadiazole (**6**), 1,4-Di(2-methyl-2-hydroxy-3-butynyl)-benzene (**7**), 1,4-di(2-methyl-2-hydroxy-3-butynyl)-benzene (**8**), 1,4-bis(2-methylbut-3-yn-2-ol)-2,5-bis(hexyloxy)benzene (**11a**), 1,4-bis(trimethylsilylethynyl)-2,5-bis(2-ethylhexyloxy)benzene (**11b**) were prepared according to the publish procedures<sup>32,33,36,37,55</sup> (details can be found in ESI).

### Synthesis of Monomer 1 - 5 and FCPs



**Scheme 2** The synthesis of monomer **1** - **5** and FCPs. Reagents and conditions: (i)  $\text{N}_2\text{H}_4\text{-H}_2\text{O}$ , PPA,  $\text{N}_2$ , 130  $^\circ\text{C}$ , 13 h; (ii)  $\text{NaNO}_2$ , HCl,  $\text{NaN}_3$ , 0-5  $^\circ\text{C}$ , 2 h; (iii) 2-methyl-3-butyn-2-ol,  $\text{Pd}(\text{Ph}_3\text{P})_4$ , CuI,  $\text{NEt}_3$ , 110  $^\circ\text{C}$ , 8 h; (iv) NaOH, toluene, reflux, 6 h; (v) TMSA,  $\text{Pd}(\text{Ph}_3\text{P})_4$ , CuI,  $\text{NEt}_3$ , 70  $^\circ\text{C}$ , 12 h; (vi)  $\text{K}_2\text{CO}_3$ , THF, 6 h; (vii) NaOH, 1-bromoalkane, NaI, reflux, 48 h; (viii) NBS,  $\text{CH}_2\text{Cl}_2/\text{CH}_3\text{COOH}$ , reflux, 24 h; (ix)  $\text{Cu}(\text{PPh}_3)_3\text{Br}$ , DMF,  $\text{N}_2$ , 12 h, 50  $^\circ\text{C}$ .

### 2,5-bis(4-azidophenyl)-1,3,4-oxadiazole (**1**)

Following the literature method (Scheme 2a),<sup>32</sup> a solution of  $\text{NaNO}_2$  (151 mg, 2.2 mmol) in water (2 mL) was added dropwise to a solution of 2,5-Bis(*p*-aminophenyl)-1,3,4-oxadiazole (252 mg, 1 mmol) in 2 N HCl (3 mL) at 0 - 5  $^\circ\text{C}$  with vigorous stirring. The mixture was kept below 5 $^\circ\text{C}$  for 30 min, the diazonium salt solution was neutralized with  $\text{CaCO}_3$ , and then a solution of  $\text{NaN}_3$  (143 mg, 2.2 mmol) in water (5 mL) was added dropwise while the



temperature was kept below 5°C. The solid precipitate was filtered and washed twice with water. Recrystallization from ethanol provided **1** as a pale yellow solid (224 mg, 74 %). The <sup>1</sup>H NMR and <sup>13</sup>C NMR spectroscopic data agreed with those published for the same compound. <sup>1</sup>H NMR (CDCl<sub>3</sub>, 500 MHz, δ ppm): 8.12 (d, *J* = 8.6 Hz, 4H), 7.17 (d, *J* = 8.6 Hz, 4H). <sup>13</sup>C NMR (CDCl<sub>3</sub>, 126 MHz, δ ppm): 163.92, 143.65, 128.58, 120.40, 119.71.

#### 1,4-diethynylbenzene (**2**)

Following the literature method (Scheme 2b),<sup>37</sup> powdered NaOH (800 mg, 20 mmol) was added to a solution of **6** (1.2 g, 5 mmol) in toluene (20 mL). The mixture was refluxed for 4 - 6 h until no acetone escaped from the reaction mixture, cooled to room temperature, and filtered. The solvent was removed under vacuum. Purification of the residue by flash chromatography provided **2** as a colourless solid (500 mg, 80 %). The <sup>1</sup>H NMR and <sup>13</sup>C NMR spectroscopic data agreed with those published for the same compound. <sup>1</sup>H NMR (CDCl<sub>3</sub>, 500 MHz, δ ppm): 3.17 (s, 2H), 7.42 (s, 4H). <sup>13</sup>C NMR (CDCl<sub>3</sub>, 126 MHz, δ ppm): 132.04, 122.59, 83.06, 79.11.

#### 1,4-diethynyl-2,5-bis(methoxy)benzene (**3**)

Following the literature method (Scheme 2c),<sup>55</sup> K<sub>2</sub>CO<sub>3</sub> (345 mg, 2.5 mmol) was added to a solution of **8** (330 mg, 1 mmol) in 5 mL THF. The reaction mixture was stirred at room temperature for 6 h and filtered to remove the solid. The solvent was removed under vacuum. Water was added to the residue, and the two phases were separated. The aqueous phase was extracted with hexane three times. The combined organic phases were dried over MgSO<sub>4</sub>, and the solvent was evaporated. The residue was purified by flash chromatography to get **3** as a white solid (135 mg, 73 %). The <sup>1</sup>H NMR and <sup>13</sup>C NMR spectroscopic data agreed with those published for the same compound. <sup>1</sup>H NMR (CDCl<sub>3</sub>, 500 MHz, δ ppm): 6.97 (s, 2H), 3.85 (s, 6H), 3.39 (s, 2H). <sup>13</sup>C NMR (126 MHz, CDCl<sub>3</sub>, δ ppm): 154.41, 116.15, 112.63, 82.83, 79.67, 54.43.

#### 1,4-diethynyl-2,5-bis(hexyloxy)benzene (**4**)

Following the literature method (Scheme 2c),<sup>36</sup> K<sub>2</sub>CO<sub>3</sub> (345 mg, 2.5 mmol) was added to a solution of **11a** (442 mg, 1 mmol) in 5 mL THF. The reaction mixture was stirred at room temperature for 6 h and filtered to remove the solid. The solvent was removed under vacuum. Water was added to the residue, and the two phases were separated. The aqueous phase was extracted with hexane three times. The combined organic phases were dried over MgSO<sub>4</sub>, and the solvent was evaporated. The residue was purified by flash chromatography to get **4** as a light yellow solid (211 mg, 65 %). The <sup>1</sup>H NMR and <sup>13</sup>C NMR spectroscopic data agreed with those published for the same compound. <sup>1</sup>H NMR (CDCl<sub>3</sub>, 500 MHz, δ ppm): 6.95 (s, 2H), 3.97 (t, *J* = 6.6 Hz, 4H), 3.33 (s, 2H), 1.83 - 1.76 (m, 4H), 1.50 - 1.44 (m, 4H), 1.37 - 1.30 (m, 8H), 0.91 - 0.89 (t, *J* = 7.1 Hz, 6H). <sup>13</sup>C NMR (126 MHz, CDCl<sub>3</sub>, δ ppm): 154.02, 117.79, 113.30, 82.41, 79.8, 69.70, 31.54, 29.11, 25.60, 22.60, 14.03.

#### 1,4-diethynyl-2,5-bis(2-ethylhexyloxy)benzene (**5**)

Following the literature method (Scheme 2c),<sup>33</sup> K<sub>2</sub>CO<sub>3</sub> (345 mg, 2.5 mmol) was added to a solution of **11b** (526 mg, 1 mmol) in 5 mL THF. The reaction mixture was stirred at room temperature for 6 h and filtered. The solvent was removed under vacuum. Water was

added to the residue, and the two phases were separated. The aqueous phase was extracted with hexane three times. The combined organic phases were dried over MgSO<sub>4</sub>, and the solvent was evaporated. The residue was purified by flash chromatography on a very short silica gel column to get **5** as light yellow oil (187 mg, 49 %). The <sup>1</sup>H NMR and <sup>13</sup>C NMR spectroscopic data agreed with those published for the same compound. <sup>1</sup>H NMR (CDCl<sub>3</sub>, 500 MHz, δ ppm): 6.95 (s, 2H), 3.85 (d, *J* = 5.8 Hz, 4H), 3.30 (s, 2H), 1.75 (m, 2H), 1.59 - 1.24 (m, 16H), 0.97 - 0.86 (m, 12H). <sup>13</sup>C NMR (126 MHz, CDCl<sub>3</sub>, δ ppm): 154.28, 117.58, 113.27, 82.31, 79.82, 72.15, 39.39, 30.52, 29.07, 23.91, 23.06, 14.09, 11.17.

### Synthesis of FCPs via Copper-Catalyzed Click Polymerization

To a 5 mL flask were added **1** (0.1 mmol), **2** (0.1 mmol), and Cu(PPh<sub>3</sub>)<sub>3</sub>Br (0.005 mmol) under nitrogen. The mixture was degassed by several cycles. Then dry DMF (1.5 mL) was injected into the flask to dissolve the monomers and catalyst. The reaction mixture was degassed one more time and the reaction flask was evacuated and flushed with argon. The reaction mixture was stirred at 50 °C for 12 h. Then, the mixture was diluted with chloroform and added drop wise to a mixture of a hexane/chloroform (10:1 by volume). The precipitate was allowed to stand overnight, then collected and dried to get FCP 1 with a yield of 37 % (Scheme 2e). By replacing monomer **2** with **3**, **4**, or **5**, FCP 2, FCP 3, and FCP 4 were synthesized by following the same procedure with a yield of 49 %, 61 %, or 67 %, respectively. FTIR (KBr) ν (cm<sup>-1</sup>): FCP 1 3296, 3106, 2127, 2092, 1610, 1508, 1490; FCP 2 3292, 3096, 2940, 2840, 2120, 2091, 1603, 1504, 1495; FCP 3 3310, 3061, 2924, 2854, 2125, 2091, 1671, 1502, 1492; FCP 4 3309, 3059, 2954, 2922, 2855, 2129, 2091, 1611, 1502, 1499.

### Acknowledgements

We thank the National Natural Science Foundation of China for financial support (NSFC21174113). The authors also thank Mr. Yihan Pei from Clare College, University of Cambridge for the help with language.

### Notes and references

Address, College of Science, Northwest A&F University, Yangling, Shaanxi 712100, People's Republic of China, Fax: +86 2987092769; Tel: +86 2987091196; E-mail: peiyx@nwfau.edu.cn

† Electronic Supplementary Information (ESI) available: Experimental procedures and additional results including fluorescence curves, NMR data and FTIR spectra. See DOI: 10.1039/b000000x/

- 1 H. T. Ratte, *Environ. Toxicol. Chem.*, 1999, **18**, 89-108.
- 2 D. S. Merrell and A. Camilli, *J. Bacteriol.*, 2000, **182**, 5342-5350.
- 3 R. Behra, L. Sigg, M. J. Clift, F. Herzog, M. Minghetti, B. Johnston, A. Petri-Fink and B. Rothen-Rutishauser, *J. R. Soc. Interface*, 2013, **10**, 20130396.
- 4 L. Liu, G. Zhang, J. Xiang, D. Zhang and D. Zhu, *Org. Lett.*, 2008, **10**, 4581-4584.
- 5 M. Kumar, R. Kumar and V. Bhalla, *Org. Lett.*, 2011, **13**, 366-369.
- 6 N. J. Wang, C. M. Sun and W. S. Chung, *Sens. Actuators B: Chem.*, 2012, **171-172**, 984-993.
- 7 H. Tong, L. X. Wang, X. B. Jing and F. S. Wang, *Macromolecules*, 2002, **35**, 7169-7171.

- 8 C. Qin, W. Wong, Yeung and L. Wang, *Macromolecules*, 2011, **44**, 483-489.
- 9 Y. Bao, Q. Li, B. Liu, F. Du, J. Tian, H. Wang, Y. Wang and R. Bai, *Chem. Commun.*, 2012, **48**, 118-120.
- 10 S. Sun, B. Qiao, N. Jiang, J. Wang, S. Zhang and X. Peng, *Org. Lett.*, 2014, **16**, 1132-1135.
- 11 Y. J. Gong, X. B. Zhang, C. C. Zhang, A. L. Luo, T. Fu, W. h. Tan, G. L. Shen and R. Q. Yu, *Anal. Chem.*, 2012, **84**, 10777-10784.
- 12 C. B. Murphy, Y. Zhang, T. Troxler, V. Ferry, J. J. Martin and W. E. Jones, *J. Phys. Chem. B*, 2004, **108**, 1537-1543.
- 13 H. C. Kolb, M. G. Finn and K. B. Sharpless, *Angew. Chem. Int. Ed.*, 2001, **40**, 2004-2021.
- 14 E. Zhao, H. Li, J. Ling, H. Wu, J. Wang, S. Zhang, J. W. Lam, J. Z. Sun, A. Qin and B. Z. Tang, *Poly. Chem.*, 2014, **5**, 2301-2308.
- 15 W. Z. Yuan, Z. Yu, Qiang, Y. Tang, J. W. Y. Lam, N. Xie, P. Lu, E. Chen, Qiang and B. Z. Tang, *Macromolecules*, 2011, **44**, 9618-9628.
- 16 S. Bakbak, P. J. Leech, B. E. Carson, S. Saxena, W. P. King and U. H. F. Bunz, *Macromolecules*, 2006, **39**, 6793-6795.
- 17 O. Plietzsch, C. I. Schilling, T. Grab, S. L. Grage, A. S. Ulrich, A. Comotti, P. Sozzani, T. Muller and S. Braese, *New J. Chem.*, 2011, **35**, 1577-1581.
- 18 A. Qin, J. W. Y. Lam, L. Tang, C. K. W. Jim, H. Zhao, J. Sun and B. Z. Tang, *Macromolecules*, 2009, **42**, 1421-1424.
- 19 G. Nagarjuna, A. Kumar, A. Kokil, K. G. Jadhav, S. Yurt, J. Kumar and D. Venkataraman, *J. Mater. Chem.*, 2011, **21**, 16597.
- 20 J. J. Bryant and U. H. Bunz, *Chem. Asian J.*, 2013, **8**, 1354-1367.
- 21 S. W. Thomas, G. D. Joly and T. M. Swager, *Chem. Rev.*, 2007, **107**, 1339-1386.
- 22 X. Huang, J. Meng, Y. Dong, Y. Cheng and C. Zhu, *Polymer*, 2010, **51**, 3064-3067.
- 23 Y. Cheng, L. Zheng, X. Huang and Y. Shen, *Synlett*, 2010, **3**, 453-456.
- 24 Y. Wu, Y. Dong, J. Li, X. Huang, Y. Cheng and C. Zhu, *Chem. Asian J.*, 2011, **6**, 2725-2729.
- 25 C. Zhu, Y. Cheng, X. Huang, Y. Dong and J. Meng, *Synlett*, 2010, **12**, 1841-1844.
- 26 Y. T. Chang, J. K. Chang, Y. T. Lee, P. S. Wang, J. L. Wu, C. C. Hsu, I. W. Wu, W. H. Tseng, T. W. Pi, C. T. Chen and C. I. Wu, *ACS Appl. Mater. Interfaces*, 2013, **5**, 10614-10622.
- 27 T. Goudreault, Z. He, Y. Guo, C. Ho, Lam, H. Zhan, Q. Wang, K. Y. Ho, Fung, K. Wong, Leung, D. Fortin, B. Yao, Z. Xie, L. Wang, W. Kwok, Ming, P. D. Harvey and W. Wong, Yeung, *Macromolecules*, 2010, **43**, 7936-7949.
- 28 T. Higashihara, H. Wu, T. Mizobe, C. Lu, M. Ueda and W. Chen, *Macromolecules*, 2012, **45**, 9046-9055.
- 29 C. S. Wang, L. O. Palsson, A. S. Batsanov and M. R. Bryce, *J. Am. Chem. Soc.*, 2006, **128**, 3789-3799.
- 30 Y. Liu, L. Zong, L. Zheng, L. Wu and Y. Cheng, *Polymer*, 2007, **48**, 6799-6807.
- 31 P. H. Aubert, M. Knipper, L. Groenendaal, L. Lutsen, J. Manca and D. Vanderzande, *Macromolecules*, 2004, **37**, 4087-4098.
- 32 J. R. Thomas, X. J. Liu and P. J. Hergenrother, *J. Am. Chem. Soc.*, 2005, **127**, 12434-12435.
- 33 M. C. Baier, J. Huber and S. Mecking, *J. Am. Chem. Soc.*, 2009, **131**, 14267-14273.
- 34 R. E. Palacios, W. S. Chang, J. K. Grey, Y. L. Chang, W. L. Miller, C. Y. Lu, G. Henkelman, D. Zepeda, J. Ferraris and P. F. Barbara, *J. Phys. Chem. B*, 2009, **113**, 14619-14628.
- 35 L. Vacareanu, I. M. Dorin and M. Grigoras, *Rev. Chim-bucharest.*, 2010, **61**, 74-77.
- 36 B. Liu, Y. Bao, F. Du, H. Wang, J. Tian and R. Bai, *Chem. Commun.*, 2011, **47**, 1731-1733.
- 37 W. Shu, C. Guan, W. Guo, C. Wang and Y. Shen, *J. Mater. Chem.*, 2012, **22**, 3075.
- 38 Y. Hou, S. Cao, L. Wang, Y. Pei, G. Zhang, S. Zhang and Z. Pei, *Poly. Chem.*, 2015, **6**, 223-227.
- 39 V. Y. Grinshtein, A. A. Strazdin and A. K. Grinvalde, *Chem. Heterocycl. Com.*, 1970, **6**, 231-239.
- 40 A. A. Zahraa and J. J. Amer, *J. Al-qadisiyah Pure Sci.*, 2011, **16**, 1-17.
- 41 Z. Khosrow, F. Khalil, S. Reza and Z. Javad, *Turk. J. Chem.*, 2003, **27**, 119-125.
- 42 A. Faeza and H. Nazik, *J. Basrah Res.*, 2014, **40**, 146-159.
- 43 M. S. Al-Ajely, H. M. Al-Ajely and A. N. Al-NaibH, *Tikrit J. Pure Sci.*, 2008, **13**, 100-106.
- 44 J. Herbich, C. Y. Hung, R. P. Thummel and J. Waluk, *J. Am. Chem. Soc.*, 1996, **118**, 3508-3518.
- 45 D. F. Eaton, *Pure Appl. Chem.*, 1988, **60**, 1107-1114.
- 46 Y. Y. Zhu, G. T. Wang, R. X. Wang and Z. T. Li, *Cryst. Growth Des.*, 2009, **9**, 4778-4783.
- 47 R. A. Bell and J. R. Kramer, *Environ. Toxicol. Chem.*, 1999, **18**, 9-22.
- 48 Z. Zhou and C. J. Fahrni, *J. Am. Chem. Soc.*, 2004, **126**, 8862-8863.
- 49 B. Valeur, *Molecular Fluorescence: Principles and Applications*; Wiley-VCH: Weinheim, Germany, 2002.
- 50 E. Blatt, A. Mau, W. Sasse and W. Sawyer, *Aust. J. Chem.*, 1988, **41**, 127-131.
- 51 J. Lakowicz, *Principals of Fluorescence Spectroscopy*, Plenum Press: New York, 1983.
- 52 V. Banjoko, Y. Xu, E. Mintz and Y. Pang, *Polymer*, 2009, **50**, 2001-2009.
- 53 L. Q. Ying and B. P. Branchaud, *Chem. Commun.*, 2011, **47**, 8593-8595.
- 54 J. Lakowicz, *Principles of Fluorescence Spectroscopy*, 2nd ed., Plenum Publishing Corporation: New York, 1999.
- 55 Z. Li, L. Liu, W. Zhang, C. Sue, Q. Li, O. S. Miljanic, O. M. Yaghi and J. F. Stoddart, *Chem. Eur. J.*, 2009, **15**, 13356-13380.